Proc. NIPR Symp. Polar Meteorol. Glaciol., 5, 76–89, 1992

CLOUD-RADIATIVE FORCING OVER THE SNOW-COVERED SURFACE AROUND ASUKA STATION, ANTARCTICA

Teruo AOKI[1] and Takashi YAMANOUCHI[2]

[1]*Meteorological Research Institute, 1–1, Nagamine, Tsukuba 305*
[2]*National Institute of Polar Research, 9–10, Kaga 1-chome, Itabashi-ku, Tokyo 173*

Abstract: Cloud-radiative forcing at the snow-covered surface in Antarctica was estimated from data of the radiation budget observation at Asuka Station (71°31′S, 24°08′E, 930 m) in 1988. Cloud-radiative forcing at the top of the atmosphere was also estimated from satellite data in December 1988. It was found that shortwave forcing was negative (cooling) at the surface and positive (heating) at the top of the atmosphere. The longwave forcing was positive both at the surface and at the top of the atmosphere. The (shortwave+longwave) forcing was positive both at the surface and at the top of the atmosphere. This is different from those in middle and the low latitudes.

The cloud-radiative forcing distributions at the top of the atmosphere in the extended region from the sea to inland were estimated from the satellite data in December 1988. The results indicated that the shortwave forcing was positive over the snow-covered region except the high inland, and negative over the sea. The longwave forcing was positive over all regions. The (shortwave+longwave) forcing was positive over the snow-covered regions except the high inland plateau, and negative over the sea.

1. Introduction

Clouds play an important role in the radiative field of the earth-atmosphere system. The variation of cloud amount changes the radiation budget at the surface and at the top of the atmosphere. This effect is called cloud-radiative forcing, and is an important climate feedback factor in climate change.

Observational studies of cloud-radiative forcing with satellite data were carried out by RAMANATHAN *et al.* (1989) and GRUBER and STOWE (1989). There are also many studies using GCM (*e. g.*, CHARLOCK and RAMANATHAN, 1985; WETHERALD and MANABE, 1986; CESS and POTTER, 1987).

Cloud-radiative forcing has two opposite effects in the shortwave (SW) and longwave (LW) radiation fields. The increase of cloud amount increases the planetary albedo and cools the earth-atmosphere system (the SW albedo effect). It also reduces the outgoing terrestrial radiation at the top of the atmosphere and warms the earth-atmosphere system (the LW greenhouse effect) (WETHERALD and MANABE, 1986). In general, the albedo effect overcomes the greenhouse effect so that the total (SW+LW) cloud-radiative forcing is negative (CHARLOCK and RAMANATHAN, 1985).

RAMANATHAN *et al.* (1989) have estimated the global distributions of cloud-radiative forcing at the top of the atmosphere from ERBE (Earth Radiation Budget

Experiment) data and obtained the result that the (SW+LW) cloud-radiative forcing was negative over most areas except snow-covered and desert regions. However, they mentioned that the clear-sky estimates over snow-covered regions were subject to large uncertainty.

In this study, cloud-radiative forcing at the surface and at the top of the atmosphere over the snow-covered surface in Antarctica were estimated from ground data in 1988 and satellite data in December 1988.

2. Definition of Cloud-Radiative Forcing

Cloud-radiative forcing CF is defined as

$$CF=F_{\mathrm{CLD}}-F_{\mathrm{CLR}}\ , \tag{1}$$

where F_{CLD} is the cloudy sky (including not only overcast but clear-sky—*i.e.*, the mean value for the period) net radiation flux and F_{CLR} is the clear-sky net radiation flux. With F_{CLD} and F_{CLR} separately expressing the shortwave net radiation flux $SW^{\downarrow-\uparrow}$ and the longwave net radiation flux $LW^{\downarrow-\uparrow}$, CF becomes:

$$CF=(SW^{\downarrow-\uparrow}_{\mathrm{CLD}}+LW^{\downarrow-\uparrow}_{\mathrm{CLD}})-(SW^{\downarrow-\uparrow}_{\mathrm{CLR}}+LW^{\downarrow-\uparrow}_{\mathrm{CLR}})\ . \tag{2}$$

Since CF is the total $(SW+LW)$ cloud-radiative forcing, we have

$$CF=CF_{\mathrm{SW}}+CF_{\mathrm{LW}}\ , \tag{3}$$

$$CF_{\mathrm{SW}}=SW^{\downarrow-\uparrow}_{\mathrm{CLD}}-SW^{\downarrow-\uparrow}_{\mathrm{CLR}}\ , \tag{4}$$

$$CF_{\mathrm{LW}}=LW^{\downarrow-\uparrow}_{\mathrm{CLD}}-LW^{\downarrow-\uparrow}_{\mathrm{CLR}}\ . \tag{5}$$

The shortwave cloud-radiative forcing CF_{SW}, longwave cloud-radiative forcing CF_{LW} and total cloud-radiative forcing CF are calculated by eqs. (4), (5) and (3), respectively.

3. Cloud-Radiative Forcing at Asuka Station

3.1. Cloud-radiative forcing at the surface

Radiation budget observations have been made at Asuka Station, Antarctica, from January to December, 1988. Asuka Station is located as shown in Fig. 1, and the surface is always covered with snow.

Figure 2 is an example of daily variations of the SW and LW radiation fluxes at Asuka Station. The downward and upward superscript arrows indicate downward and upward fluxes, respectively. The daily mean radiation fluxes and daily mean cloud amount are shown in Table 1 on each day. The sky condition from the afternoon of December 6 to noon of December 7 was overcast by the middle cloud and sometimes snowfall was observed. On the other hand, the sky condition on December 9 was clear. The differences of both conditions in SW downward flux, SW upward flux and SW net flux were small. However, the differences of both conditions in LW downward flux and LW net flux were larger than those for SW. That is, the cloud influence on the LW radiation budget was greater than that on the SW radiation budget.

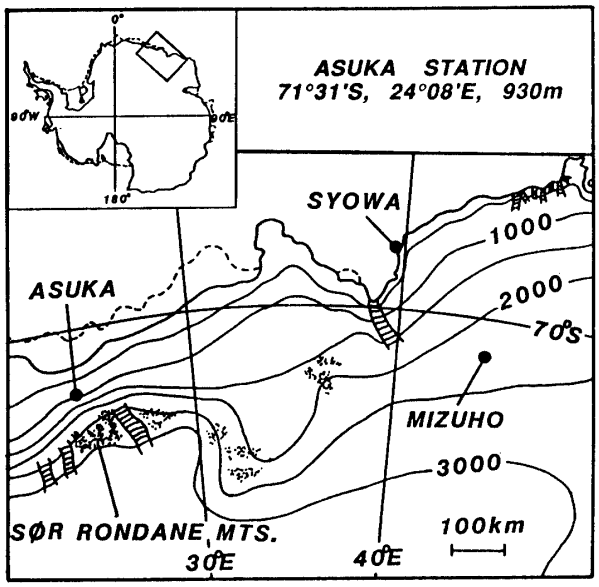

Fig. 1. Location map of Asuka Station and the extended regions where cloud-forcing at the top of the atmosphere have been estimated.

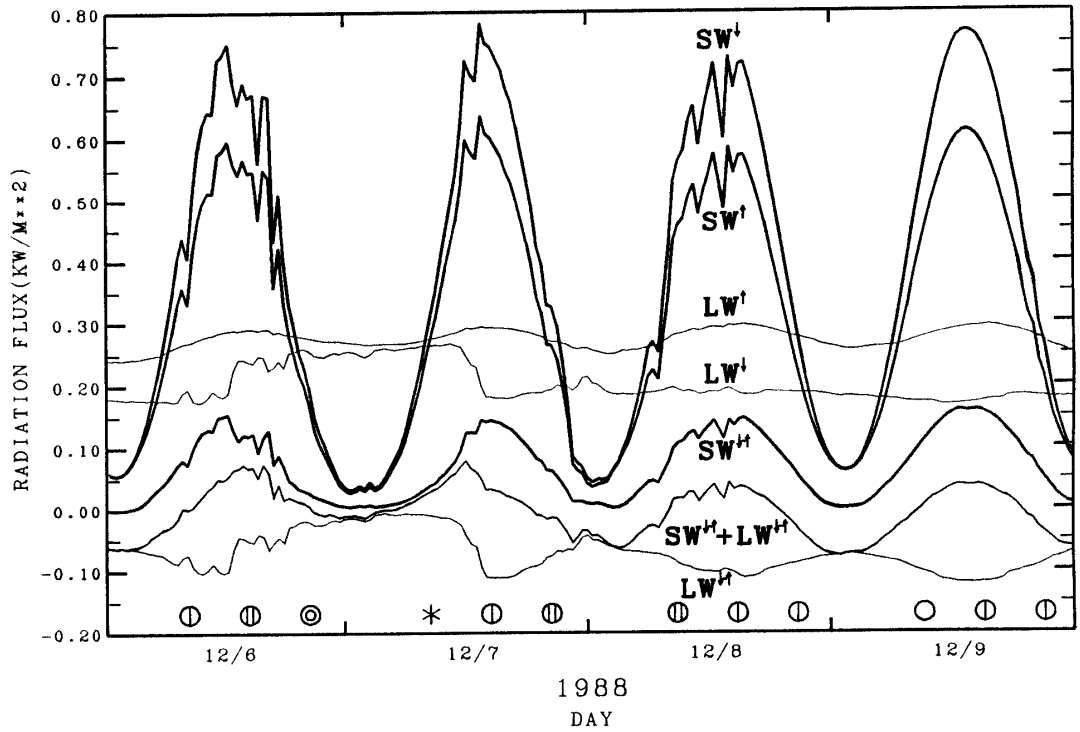

Fig. 2. Example of the daily variations of 30-min mean radiation fluxes at Asuka Station (December 6–9, 1988). SW and LW indicate shortwave and longwave radiation fluxes, respectively. The downward and the upward superscript arrows indicate downward and upward fluxes. The symbols in the figure indicate the weather observed visually.

Figure 3 shows the relationships between the daily mean cloud amounts obtained from visual observation and the daily mean radiation fluxes in December 1988. When the cloud amount increases, the SW net flux decreases and the LW net flux increases. This means that the SW forcing was negative and the LW forcing was positive. Since

Table 1. Daily mean radiation fluxes (W/m^2) from December 6 to 9, and daily mean cloud amount ($\bar{N}$).

	Dec. 6	Dec. 7	Dec. 8	Dec. 9
$SW\downarrow$	0.355	0.346	0.385	0.408
$SW\uparrow$	0.293	0.286	0.312	0.329
$SW\downarrow-\uparrow$	0.062	0.060	0.073	0.080
$LW\downarrow$	0.211	0.226	0.189	0.176
$LW\uparrow$	0.270	0.276	0.275	0.273
$LW\downarrow-\uparrow$	−0.059	−0.050	−0.086	−0.097
$SW\downarrow-\uparrow+LW\downarrow-\uparrow$	0.003	0.010	−0.013	−0.017
$\bar{N}$	9.3	9.0	5.7	3.7

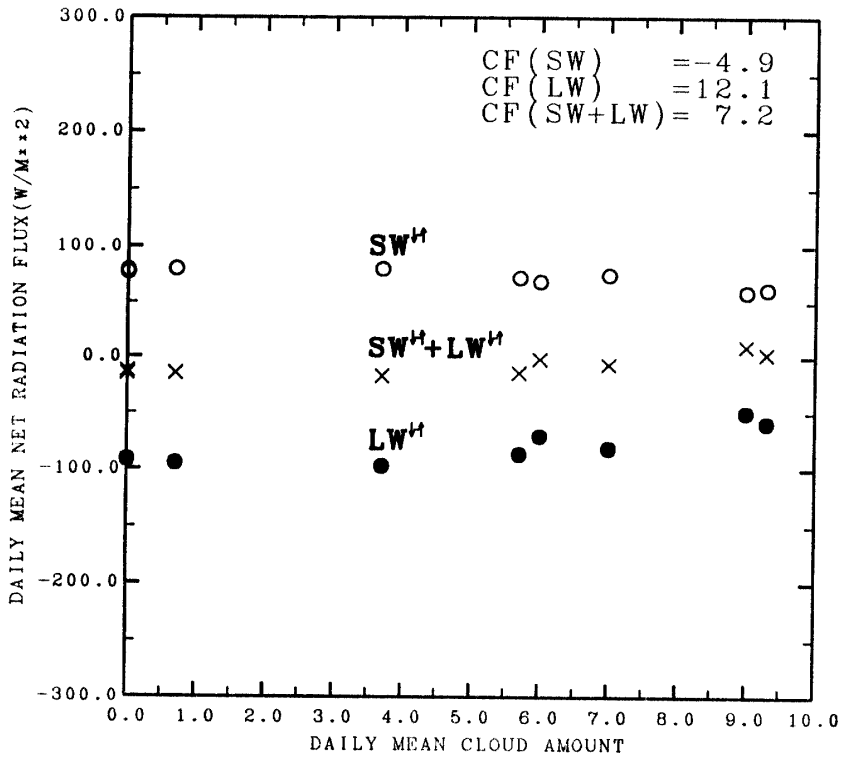

Fig. 3. Relationships between daily mean observed cloud amounts and daily mean net radiation fluxes (W/m^2) at Asuka Station in December 1988.

the absolute value of cloud forcing for LW was larger than that for SW, the total (SW+LW) forcing was positive. In eqs. (4) and (5), the values of $SW^{\downarrow-\uparrow}_{CLR}$ and $LW^{\downarrow-\uparrow}_{CLR}$ are means of the daily mean fluxes in the case of daily mean cloud amount less than 1.5. On the other hand, the values of $SW^{\downarrow-\uparrow}_{CLD}$ and $LW^{\downarrow-\uparrow}_{CLD}$ are montly means of daily mean fluxes. The results were obtained as $CF_{SW}=-4.9$ W/m^2, $CF_{LW}=12.1$ W/m^2 and $CF=7.2$ W/m^2 in December 1988.

The SW forcing given by eq. (4) can be rewritten by using the surface albedo in the form

$$CF_{SW}=(1-a_{CLD})SW^{\downarrow}_{CLD}-(1-a_{CLR})SW^{\downarrow}_{CLR}\ , \qquad (6)$$

where a_{CLD}, a_{CLR} are the surface albedos for cloudy and clear sky, respectively. Since cloud cover makes the SW downward flux decrease (we call this the "shade effect" here), we can obtain the following relation:

$$SW^{\downarrow}_{CLD} < SW^{\downarrow}_{CLR} . \tag{7}$$

The daily mean shortwave downward fluxes on December 7 (cloudy) and December 9 (clear) were 0.346 W/m^2 and 0.408 W/m^2, respectively, as shown in Table 1. The difference between these two values is 0.062 W/m^2, which is only 15% of 0.408 W/m^2. At Asuka Station, the decrease of downward shortwave flux by cloud cover never exceeded 50% as in middle and low latitudes. The reason is considered to be that the cloud cover over Asuka Station is optically thin and multiple reflections between the cloud and snow surface occurred. Moreover, cloud cover also makes the surface albedo increase ($\sim$5%) as reported by YAMANOUCHI (1983), so we obtained the following:

$$(1-a_{CLD}) < (1-a_{CLR}) . \tag{8}$$

From eqs. (7) and (8), the relation between the first term and the second term on the right-hand side of eq. (6) is given by

$$(1-a_{CLD})SW^{\downarrow}_{CLD} < (1-a_{CLR})SW^{\downarrow}_{CLR} .$$

Thus, we finally obtained the following relation:

$$CF_{SW} < 0 . \tag{9}$$

The LW forcing given by eq. (5) is rewritten in the form

$$CF_{LW} = (LW^{\downarrow}_{CLD} - LW^{\downarrow}_{CLR}) - (LW^{\uparrow}_{CLD} - LW^{\uparrow}_{CLR}) . \tag{10}$$

Since cloud cover makes the LW downward flux increase (greenhouse effect), we have

$$LW^{\downarrow}_{CLD} - LW^{\downarrow}_{CLR} > 0 . \tag{11}$$

The LW downward flux under cloudy (including snowfall) conditions was 0.07$\sim$0.08 W/m^2 larger than that under clear conditions, as shown in Fig. 2. Moreover, cloud-cover (which increases LW downward flux) warms the surface, and the LW upward flux also increases due to the rise of the surface temperature, so we have

$$LW^{\uparrow}_{CLD} - LW^{\uparrow}_{CLR} > 0 . \tag{12}$$

However, the difference of the LW upward fluxes between cloudy and clear conditions was very small, as shown in Fig. 2. Since the increase of the LW downward flux by cloud cover (eq. (11)) overcomes that for the LW upward flux (eq. (12)), we have

$$(LW^{\downarrow}_{CLD} - LW^{\downarrow}_{CLR}) > (LW^{\uparrow}_{CLD} - LW^{\uparrow}_{CLR}) .$$

Thus,

$$CF_{LW} > 0 . \tag{13}$$

The SW negative forcing is mainly caused by the shade effect, and the LW positive

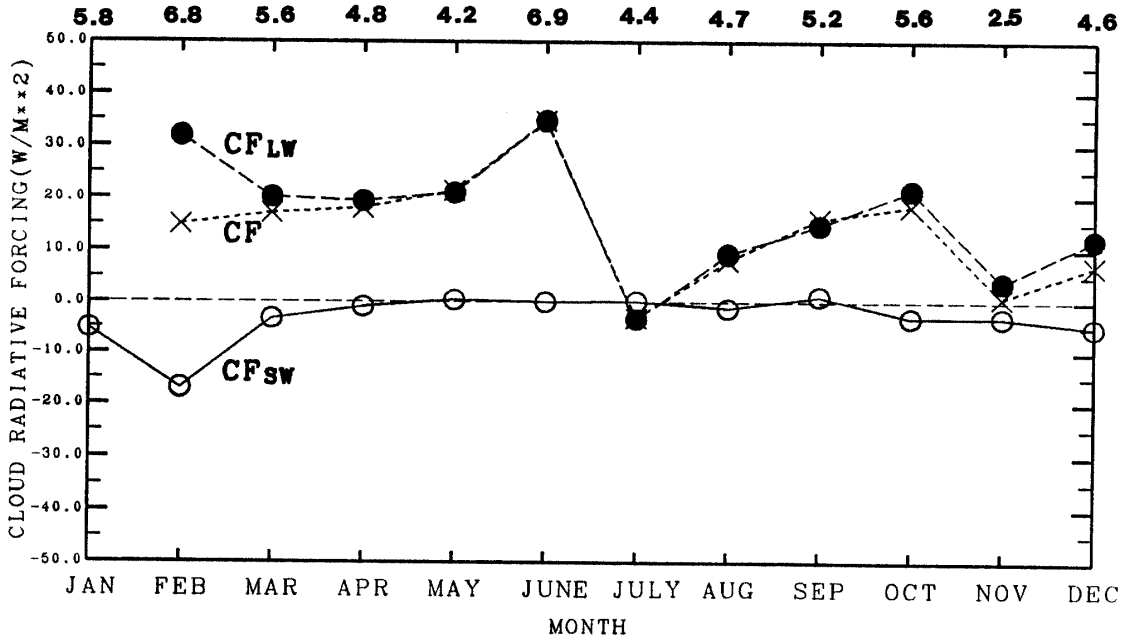

Fig. 4. Seasonal variations of cloud-radiative forcing (W/m^2) at Asuka Station in 1988. The values above the figure are monthly mean cloud amounts.

forcing is mainly caused by the greenhouse effect. Since the latter overcomes the former, the total forcing was positive. This phenomenon is known as the "radiation paradox": the decrease in the shortwave net flux with increasing cloudiness is over-compensated by increased longwave net flux over a high albedo surface, as discussed by AMBACH (1974) and WENDLER (1986).

The seasonal variations of cloud-radiative forcing are shown in Fig. 4. The SW forcing had negative values, and the LW forcing and total forcing had positive values, in most months. Since the polar night at Asuka Station was from May 20 to July 20 in 1988, the *SW* forcing in May, June and July was close to zero.

3.2. Cloud-radiative forcing at the top of the atmosphere

Cloud-radiative forcing at the top of the atmosphere over Asuka Station was estimated from the NOAA AVHRR (Advanced Very High Resolution Radiometer) data in December 1988. The NOAA data were received and processed at Syowa Station (69°00'S, 39°35'E). This receiving and processing system was discussed by TAKABE and YAMANOUCHI (1989). One image per day has been used for each channel (Ch. 1–Ch. 5). Since the areas observed by the NOAA satellite changed day by day, they were adjusted by using the landmark of Sør Rondane Mountains located south of Asuka Station (Fig. 1). The resolution of field of view in one pixel was 2.2 km. Daily channel data were averaged 5×5 pixels around Asuka Station.

The shortwave broadband planetary albedos were estimated from the narrowband planetary albedos on Ch. 1 (0.58–0.68 μm) and Ch. 2 (0.73–1.1 μm) on NOAA AVHRR following WYDICK *et al.* (1987) and given as

$$\alpha=A_0+\alpha_1A_1+\alpha_2A_2\ , \tag{14}$$

where α_1 and α_2 are the narrowband planetary albedos of Ch. 1 and Ch. 2, respectively. The constants A_0, A_1 and A_2 are $A_0=0.746$, $A_1=0.347$ and $A_2=0.650$. These coefficients were empirically derived through multivariant regression analysis of Nimbus-7 ERB (Earth Radiation Budget) broadband data and NOAA-7 AVHRR Ch. 1 and Ch. 2 narrowband data for the various surfaces including ocean, cloud and snow. The shortwave net radiation flux SW is expressed as

$$SW^{\downarrow-\uparrow}=(1-\alpha)S_0\cos\theta_0\,, \tag{15}$$

where S_0 is the extraterrestrial solar constant, and θ_0 is the daily mean solar zenith angle.

Since the downward longwave radiation flux $LW^{\downarrow}$ is zero at the top of the atmosphere, $LW^{\downarrow-\uparrow}$ can be expressed as

$$LW^{\downarrow-\uparrow}=-LW^{\uparrow}. \tag{16}$$

$LW^{\uparrow}$ is related to the broadband longwave brightness temperature T_f given as

$$LW^{\uparrow}=\sigma T_f^4\,, \tag{17}$$

where σ is the Stephan-Boltzmann constant. Also T_f was estimated from the infrared window brightness temperature of Ch. 4 (10.3–11.3 μm) and Ch. 5 (11.5–12.5 μm) on NOAA AVHRR following OHRING and GRUBER (1984) and given as

$$T_f=aT_W+bT_W^2\,, \tag{18}$$

where T_W is the mean brightness temperature of Ch. 4 and Ch. 5, and the coefficients a and b were obtained by ELLINGSON and FERRARO (1983), as reported by OHRING and GRUBER (1984), as $a=1.2736$ and $b=-1.231\times10^{-3}$. These coefficients were also empirically derived through quadratic regression analysis of Nimbus ERB data and NOAA 10 μm window data. Cloud amounts were estimated by visual observation at 1500 LT, which was approximately the passage time of the satellite.

The relationships between cloud amounts and the net radiation fluxes are shown in Fig. 5. The SW forcing, LW forcing and total forcing at the top of the atmosphere were calculated by eqs. (3)~(5) and the same condition as those at the surface. The results were obtained as $CF_{SW}=12.8$ W/m^2, $CF_{LW}=10.3$ W/m^2 and $CF=23.1$ W/m^2 in December 1988. The positive SW forcing was different from the result on the surface. At the top of the atmosphere, the SW forcing equation has a similar form to eq. (6):

$$CF_{SW}=(1-a_{CLD})S_0\cos\theta_0-(1-a_{CLR})S_0\cos\theta_0\,,$$

where a_{CLD} and a_{CLR} are the planetary albedos for cloudy and clear sky, respectively, S_0 is the extraterrestrial solar constant, and θ_0 is the solar zenith angle. Thus, we obtained

$$CF_{SW}=(a_{CLR}-a_{CLD})S_0\cos\theta_0\,. \tag{19}$$

Equation (19) means that the SW forcing is determined by the planetary albedo.

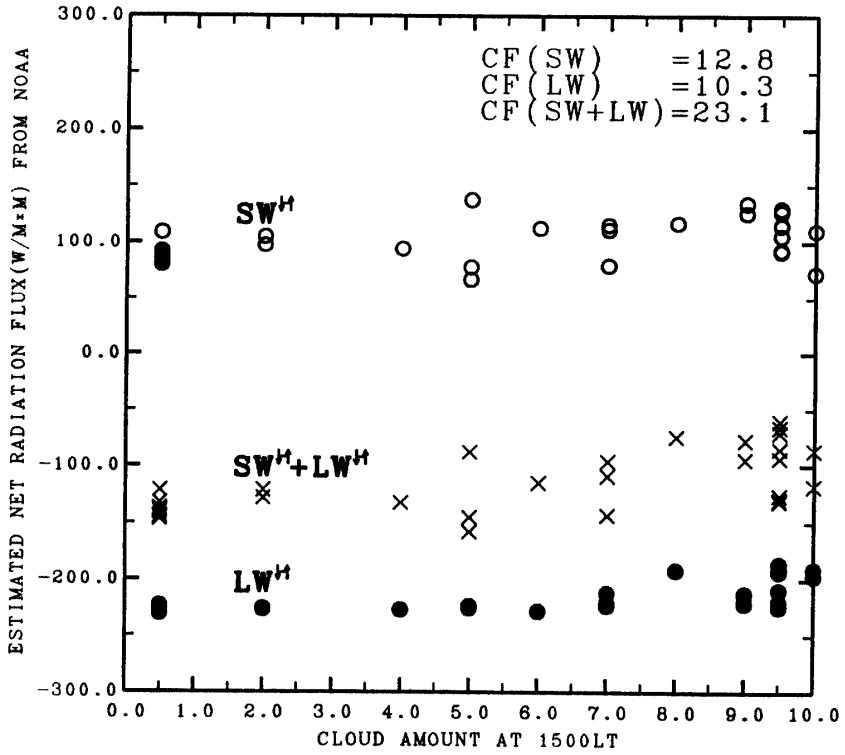

Fig. 5. Relationships between cloud amounts and the net radiation fluxes (W/m^2) estimated from NOAA data at the top of the atmosphere over Asuka Station in December 1988. Cloud amounts are the values of visual observations 1500 LT at Asuka Sation.

Therefore, the positive SW forcing means that cloud cover makes the planetary albedo decrease. This phenomenon can be explained when clouds absorbing the shortwave radiation appear on a high albedo surface. Clouds with little absorption may make the planetary albedo increase. In Fig. 5, the circles of the shortwave net flux appear to be independent on cloud amount. This is considered to be because various types of clouds (absorbing and little absorbing) appear over Asuka Station. We can calculate the SW forcing by eq. (4), whether the shortwave upward flux depends on cloud amount or not. The positive forcing we obtained here is only the result in December 1988 and is not a universal result for the other months or years. The sign of the SW forcing may change easily according to the kind of clouds which appear.

On the other hand, the LW forcing was positive. At the top of the atmosphere, the LW forcing equation is given by

$$CF_{\mathrm{LW}}=LW^{\uparrow}_{\mathrm{CLR}}-LW^{\uparrow}_{\mathrm{CLD}}\ . \tag{20}$$

From eq. (20), the positive LW forcing means that cloud cover makes the LW upward flux decrease. This is a greenhouse effect of the clouds.

Since both the SW and LW forcing were positive, the total forcing was also positive.

4. Cloud-Radiative Forcing at the Top of the Atmosphere in the Extended Regions

Asuka Station is only one point in vast Antarctica. Therefore, it is not known whether cloud-radiative forcing at Asuka Station represents that over the coastland and/or inland. So the cloud-radiative forcing distribution at the top of the atmosphere in the extended regions shown in Fig. 1 was estimated from the satellite data in December 1988.

It is difficult to detect cloud cover in polar regions. Since the ground surface temperature is very low, the contrast in the visible albedo and the infrared brightness temperature is very small between the surface and the cloud top as mentioned by YAMANOUCHI *et al.* (1987). They discussed a method to detect cloud cover in the Antarctic using Ch. 3 (3.5–3.9 μm), Ch. 4 and Ch. 5 for the NOAA AVHRR data. The brightness temperatures of Ch. 3 and Ch. 4 show a positive difference when cloud thickness is in some particular range, and then tend to show a negative difference for thick clouds. Thin clouds have a difference in brightness temperature between Ch. 4 and Ch. 5 (YAMANOUCHI *et al.*, 1987). These differences were used to detect clear sky regions.

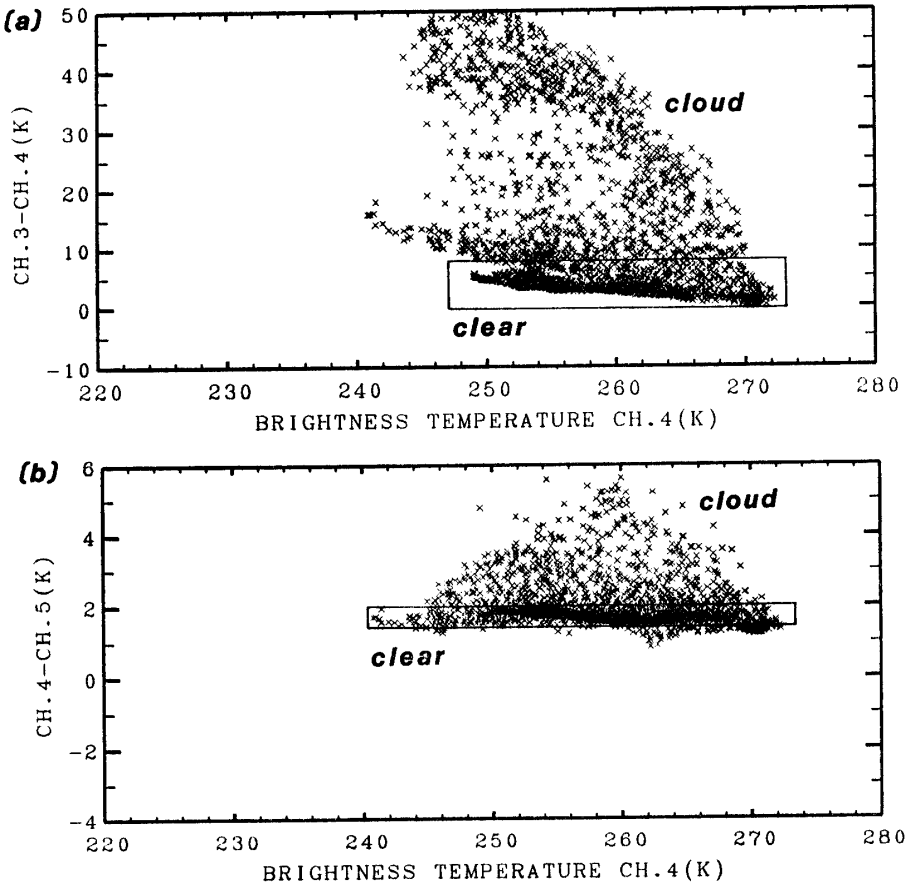

Fig. 6. Brightness temperature differences Ch. 3–Ch. 4(a) and Ch. 4–Ch. 5(b) against Ch. 4 brightness temperature in December 1988. Means of 8×8 pixels (17.6×17.6 km) in the area shown in Fig. 1.

The relations of the brightness temperature differences Ch. 3–Ch. 4 and Ch. 4–Ch. 5 against the Ch. 4 brightness temperature are shown in Fig. 6. The clear sky and the cloud cover data points are mainly distributed as indicated in Fig. 6. The clear sky areas were determined as follows. The brightness temperature differences Ch. 3–Ch. 4 and Ch. 4–Ch. 5 were averaged over 8×8 pixel (17.6×17.6 km) sub-areas in all regions. The sub-areas where Ch. 3–Ch. 4$<$10.0 and Ch. 4–Ch. 5$<$2.0 are judged as clear sky, though with a little uncertainty. For example, both brightness temperature differences Ch. 3–Ch. 4 and Ch. 4–Ch. 5 have similar values both for clear sky and for cloud cover when the Ch. 4 brightness temperature is higher than 270 K, so that cloud-covered sub-areas are judged as clear sky when the temperature is higher than 270 K on Ch. 4. When thick cloud appears, both brightness temperature differences Ch. 3–Ch. 4 and Ch. 4–Ch. 5 decrease or show negative values. Then the cloud-covered sub-areas are judged as clear sky.

The daily SW and LW net fluxes were calculated by the same method as those at the top of the atmosphere at Asuka Station. The values of $SW^{\downarrow-\uparrow}_{\mathrm{CLR}}$ and $LW^{\downarrow-\uparrow}_{\mathrm{CLR}}$ are the means of sub-areas which are judged as clear sky by the rule mentioned above, and the values of $SW^{\downarrow-\uparrow}_{\mathrm{CLD}}$ and $LW^{\downarrow-\uparrow}_{\mathrm{CLD}}$ are the monthly means of sub-areas. Consequently, cloud-radiative forcings give means for 8×8 pixel sub-areas. The SW forcing, LW forcing and total forcing distributions are shown in Figs. 7–9, respectively.

The SW forcing was negative over the sea, the high inland plateau and rocky mountains. On the other hand, the SW forcing was positive over continental regions except the high inland plateau and rocky mountains. Since the surface albedo is low over the sea and rocky mountains regions, cloud cover makes the planetary albedo increase (the albedo effect). So negative SW forcing is reasonable in these regions.

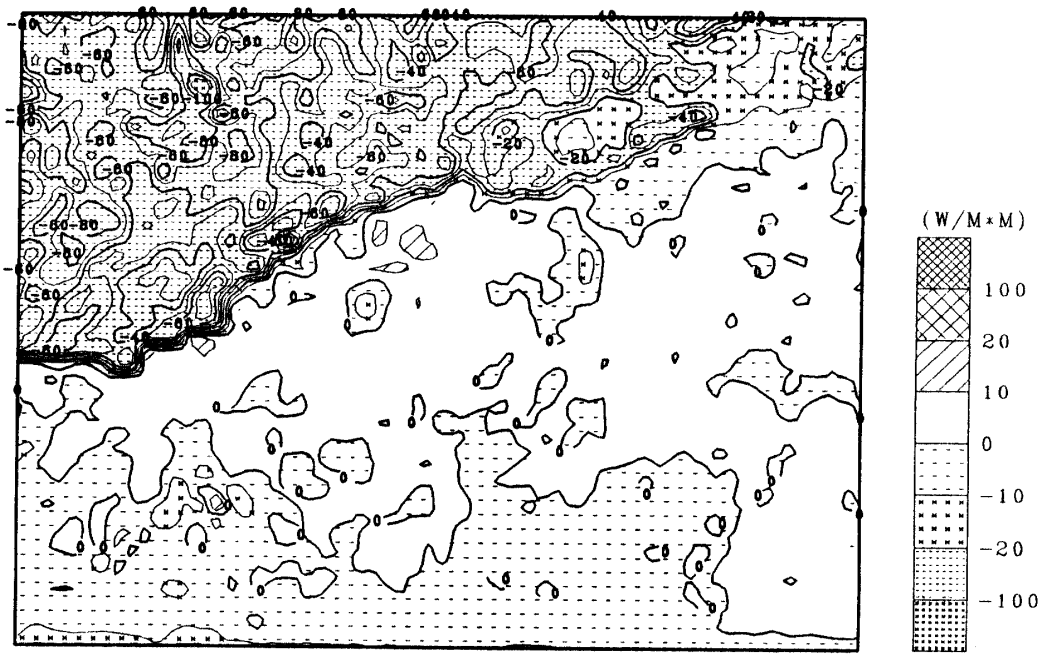

Fig. 7. Shortwave cloud-radiative forcing (W/m^2) at the top of the atmosphere in the area shown in Fig. 1 in December 1988.

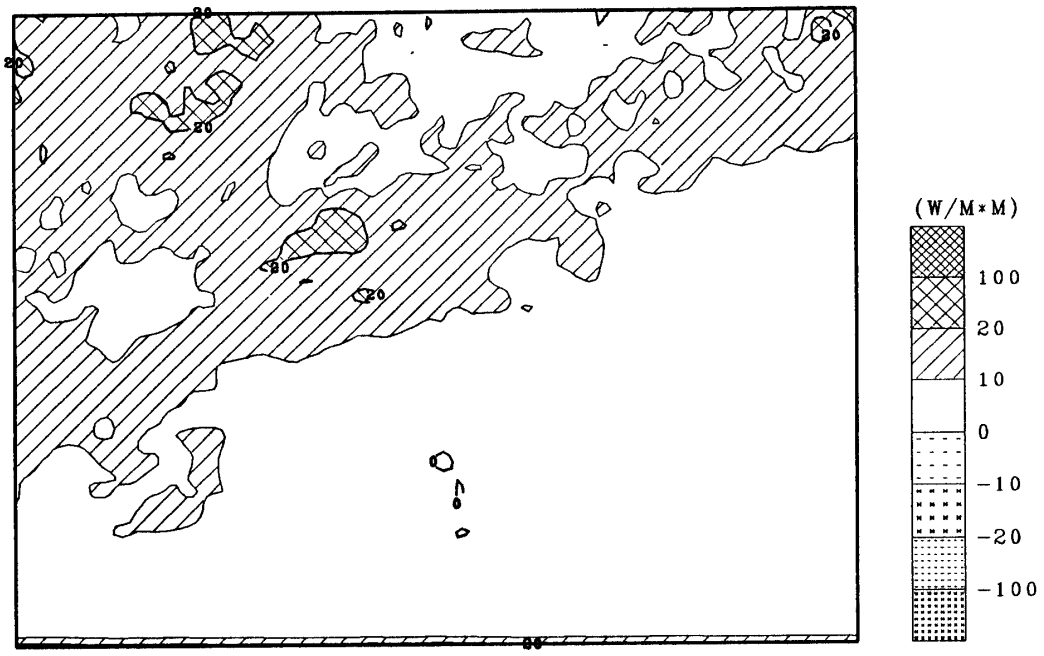

Fig. 8. Same as Fig. 7, but for the longwave cloud-radiative forcing.

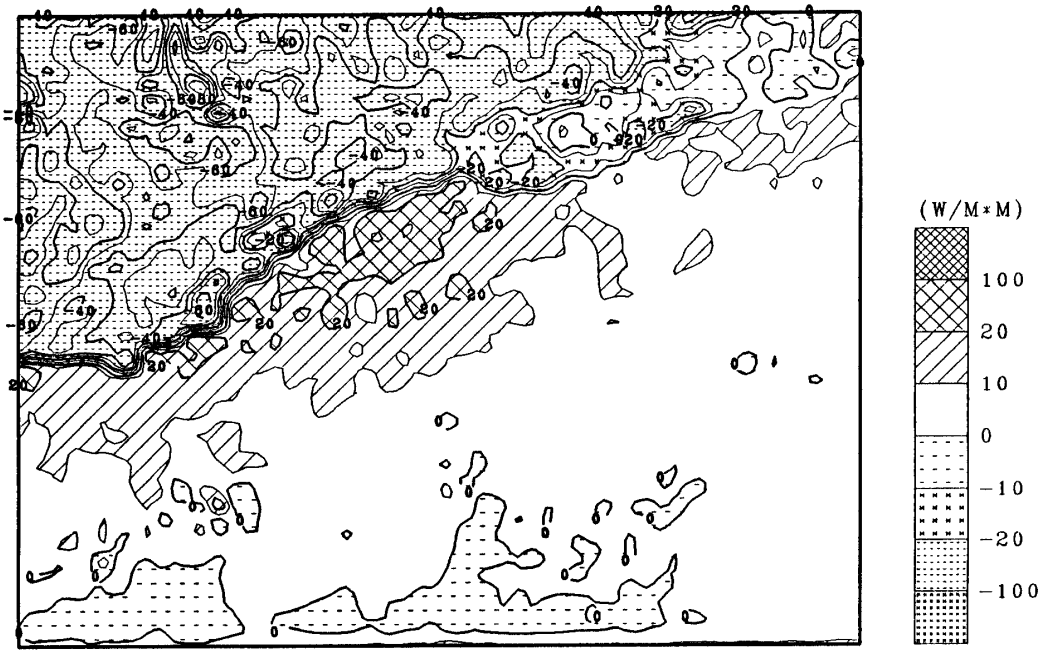

Fig. 9. Same as Fig. 7, but for the total (shortwave+longwave) cloud-radiative forcing.

The absolute value of this negative SW forcing was very large (>40 W/m^2) over the sea and small (~10 W/m^2) over rocky mountains. On the other hand, positive SW forcing was estimated over snow-covered continental regions except the high inland plateau, and negative SW forcing over the high inland plateau. This negative region corresponds well to the region where the altitude is over 3000 m shown in Fig. 1. As mentioned in the case of SW forcing at the top of the atmosphere at Asuka Station,

the reason for the positive SW forcing might be related to the appearance of clouds absorbing shortwave radiation. If clouds with absorption often appear over continental regions with elevation lower than 3000 m, and clouds with little absorption appear over the high inland plateau, the sign of the SW forcing over the continental regions can be successfully explained. Moreover, if the clouds with absorption are snow clouds, and the clouds with little absorption are cirrus, it is suggested that lows cross the area with elevation lower than 3000 m. However, the positive SW forcing was small (<10 W/m^2), and the absolute value of the negative SW forcing was still smaller (<5 W/m^2).

The LW forcing was positive in most regions due to the greenhouse effect of clouds. Its value was large (10–20 W/m^2) over the sea and was very small (<5 W/m^2) over inland. The reason is that the temperature difference between the cloud tops and the surface over inland where the altitude is high as shown in Fig. 1 is smaller than that over sea. So it can be said that the LW forcing depends on the surface altitude or surface temperature.

The total forcing was positive over regions except for the sea and the high inland plateau. These positive regions are snow-covered. This positive forcing was large over the coastland (>20 W/m^2) and small over inland (<10 W/m^2). Both the SW forcing and the LW forcing were positive in these regions; this is a characteristic phenomenon in Antarctica. On the other hand, the negative SW forcing overcomes the positive LW forcing over the sea, so the total forcing was negative, as in middle and low latitudes, and its absolute value was large (>20 W/m^2). Over the high inland plateau the negative total forcing was estimated. However, its absolute value was close to zero.

5. Summary

Cloud-radiative forcing at the surface and at the top of the atmoshere over the snow-covered surface in Antarctica were estimated from ground and satellite data in 1988.

The results at the surface indicated that the SW forcing was negative, while the LW forcing and total forcing were positive in most months in 1988. The negative SW forcing and the positive LW forcing are mainly due to the shade effect and the greenhouse effect of cloud, respectively. Since the latter overcomes the former, the total forcing was positive, which is different from what happens in middle and low latitudes.

The results at the top of the atmosphere indicated that the SW forcing, LW forcing and total forcing were all positive in December 1988. The positive SW forcing can be explained by noting that clouds which absorb shortwave radiation make the planetary albedo decrease over the high albedo snow-covered surface. The positive LW forcing is due to the greenhouse effect of cloud that makes the upward LW flux decrease.

The cloud-radiative forcing distribution at the top of the atmosphere in the extended region was estimated from satellite data in December 1988. The results indicated that the SW forcing was negative over the sea, the high inland plateau (>3000

m) and rocky mountains, and was positive over continental regions with elevation lower than 3000 m. The negative SW forcing is due to the albedo effect of cloud; its absolute value was very large (>40 W/m^2) over the sea and very small (<5 W/m^2) over the high inland plateau. The positive SW forcing can be explained by the same argument used for the forcing at the top of the atmosphere at Asuka Station; its value was small (<10 W/m^2).

In addition, the negative SW forcing was estimated over the high inland plateau (>3000 m). This can be explained by the appearance of little absorbing clouds in this region. The LW forcing was positive in most regions, due to the greenhouse effect. Its value was large (10–20 W/m^2) over the sea and small (<5 W/m^2) over the inland plateau. The total forcing was positive over most of the snow-covered regions, with large negative value (>20 W/m^2) over the sea and a small negative value (<5 W/m^2) over the high inland plateau. In these positive regions, both the SW forcing and the LW forcing were positive, which is characteristic of Antarctica. On the other hand, the negative SW forcing overcomes the positive LW forcing over the sea, so the total forcing was negative, as in middle and low latitudes.

Acknowledgments

The authors would like to thank the wintering members of JARE-29 at Asuka Station for their field assistance and Dr. K. SEKO of Nagoya University for providing the NOAA satellite data. The authors are indebted to Dr. Tadao AOKI and Dr. M. FUKABORI for assistance in preparing the manuscript.

References

AMBACH, W. (1974): The influence of cloudiness on the net radiation balance of a snow surface with high albedo. J. Glaciol., **13**, 73–84.

CESS, R. D. and POTTER, G. L. (1987): Exploratory studies of cloud radiative forcing with general circulation model. Tellus, **39A**, 460–473.

CHARLOCK, T. P. and RAMANATHAN, V. (1985): The albedo field and cloud radiative forcing produced by a general circulation model with internally generated cloud optics. J. Atmos. Sci., **42**, 1408–1429.

ELLINGSON, R. G. and FERRARO, R. R. (1983): An examination of a technique for estimating the longwave radiation budget from satellite radiation observations. J. Climate Appl. Meteorol., **22**, 1416–1423.

GRUBER, A. and STOWE, L. L. (1989): An analysis of cloud radiation forcing as calculated from ERBE, AVHRR and Nimbus-7 ERB and cloud data. Adv. Space Res., **9**, 129–139.

OHRING, G. and GRUBER, A. (1984): Satellite determinations of the relationship between total longwave radiation flux and infrared window radiance. J. Climate Appl. Meteorol., **23**, 416–425.

RAMANATHAN, V., CESS, R. D., HARRISON, E. F., MISSIS, P., BARKSTROM, B. R., AHMAD, E. and HARTHMANN, D. (1989): Cloud-radiative forcing and climate: Results from the earth radiation budget experiment. Science, **243**, 57–63.

TAKABE, H. and YAMANOUCHI, T. (1989): Kishô eisei NOAA dêta shori sôchi (NOAA data processing system). Nankyoku Shiryô (Antarct. Rec.), **33**, 73–87.

WENDLER, G. (1986): The "Radiation Paradox" on the slopes of the Antarctic continent. Polarforschung, **56**, 33–41.

WETHERALD, R. T. and MANABE, S. (1986): An investigation of cloud cover change in response to

thermal forcing. Climate Change, **8**, 5–23.

WYDICK, J. E., DAVIS, P. A. and GRUBER, A. (1987): Estimation of broadband planetary albedo from operational narrowband satellite measurements. NOAA Tech. Rep., NESDIS, **27**, 32 p.

YAMANOUCHI, T. (1983): Variations of incident solar flux and snow albedo on the solar zenith angle and cloud cover, at Mizuho Station, Antarctica. J. Meteorol. Soc. Jpn., **61**, 879–893.

YAMANOUCHI, T., SUZUKI, K. and KAWAGUCHI, S. (1987): Detection of clouds in Antarctica from infrared multispectral data of AVHRR. J. Meteorol. Soc. Jpn., **65**, 949–962.

(Received November 10, 1990; Revised manuscript received April 9, 1991)